Mesoporous Sieves with Unified Hybrid Inorganic/Organic Frameworks

Brian J. Melde, Brian T. Holland, Christopher F. Blanford, and Andreas Stein*

Department of Chemistry, University of Minnesota, Minneapolis, Minnesota 55455

Received June 22, 1999. Revised Manuscript Received August 30, 1999

Mesoporous materials have been synthesized that are composed of hybrid frameworks in which inorganic and organic components have a fixed stoichiometry and are covalently bonded. The creation of UOFMN (unified organically functionalized mesoporous networks) materials incorporates concepts employed in the synthesis of MCM-41 mesoporous silicates, making use of a quaternary ammonium cationic surfactant and a double trialkoxysilyl precursor such as bis(triethoxysilyl)ethane (BTSE) or bis(triethoxysilyl)ethylene (BTSEY). The cetyltrimethylammonium (CTA^+) surfactant is removed by extraction with acid, resulting in a high surface area porous organosilicate framework in which Si atoms are bridged by ethane (from BTSE) or ethylene (BTSEY) groups. The channels are wormlike and uniform in diameter. UOFMN materials are more hydrothermally stable than MCM-41 prepared under similar conditions and have thicker pore walls. Ethylene groups in products made with BTSEY can be brominated, the brominated product itself being reactive as a bromide source. The UOFMN products were characterized by XRD, N_2 adsorption, solid-state ^{29}Si and ^{13}C NMR, and TEM.

Introduction

A major breakthrough in the synthesis of high surface area mesoporous materials came in 1992 with the report of MCM-41, a hexagonally ordered porous silicate or aluminosilicate with a narrow pore size distribution.[1,2] The synthesis of MCM-41 combines surfactant micelles which act as space fillers and a silicate source which, for example, may be a tetraalkoxysilane. Many studies have been conducted to discover ordered mesoporous materials of differing metal oxide compositions, as well as hybrid inorganic/organic structures. Hybrid MCM-41-type products reported thus far have been inorganic structures with surfaces modified with organic functional groups. One approach to surface modification is postsynthesis grafting. Groups that have been grafted onto MCM-41 include amino groups,[3,4] organometallic lanthanide silylamides,[5] thiol groups,[6−8] epoxides,[9,10] and ferrocenyl groups.[11] Hybrid products can also result from a direct synthetic approach in which more than one precursor is combined, for example, tetraethoxysilane (TEOS) with vinyltriethoxysilane to form a vinyl functionalized MCM-41.[12] Other hybrid products created by this method include ordered porous silicates functionalized with thiol,[13,14] phenyl,[15] aminopropyl,[16] and methacrylate[17] groups.

The production of hybrid inorganic/organic materials that are not necessarily ordered but perhaps have novel properties has been recently reviewed.[18] Hybrid materials can be synthesized by sol−gel methods based on inorganic polymerization reactions, such as the hydrolysis and condensation of metal alkoxides. Originally used for the production of glasses and ceramics, sol−gel methods have proven to be beneficial for syntheses of compositionally controlled hybrid inorganic/organic materials. Low molecular weight organic compounds can be consolidated with inorganic species at temperatures under which the organic components can survive. Hybrid products have been called "ceramers"[19] and "ormocers"[20] (organically modified ceramics). Such materials may have unique combinations of properties not obtained by those of organic or inorganic composition alone, properties which may be useful for electrical, optical,[21−25] or coating[25−31] applications.

(1) Kresge, C. T.; Leonowicz, M. E.; Roth, W. J.; Vartuli, J. C.; Beck, J. S. *Nature* **1992**, *359*, 710−712.
(2) Beck, J. S.; Vartuli, J. C.; Roth, W. J.; Leonowicz, M. E.; Kresge, C. T.; Schmitt, K. D.; Chu, C. T.-W.; Olson, D. H.; Sheppard, E. W.; McCullen, S. B.; Higgins, J. B.; Schlenker, J. L. *J. Am. Chem. Soc.* **1992**, *114*, 10834−10843.
(3) Cauvel, A.; Renard, G.; Brunel, D. *J. Org. Chem.* **1997**, *62*, 749−751.
(4) Diaz, J. F.; K. J. Balkus, J. *Chem. Mater.* **1997**, *9*, 61−67.
(5) Anwander, R.; Roesky, R. *J. Chem. Soc., Dalton Trans.* **1997**, 137−138.
(6) Mercier, L.; Pinnavaia, T. J. *Adv. Mater.* **1997**, *9*, 500.
(7) Feng, X.; Fryxell, G. E.; Wang, L. Q.; Kim, A. Y.; Liu, J.; Kemner, K. M. *Science* **1997**, *276*, 923.
(8) Liu, J.; Feng, X.; Fryxell, G. E.; Wang, L. Q.; Kim, A. Y. *Adv. Mater.* **1998**, *10*, 161.
(9) Rao, Y. S.; Vos, D. E. D.; Bein, T.; Jacobs, P. A. *Chem. Commun.* **1997**, 355.
(10) Rao, Y. V. S.; Vos, D. E. D.; Bein, T.; Jacobs, P. A. *Angew. Chem., Int. Ed. Engl.* **1997**, *36*, 2661.
(11) O'Brien, S.; Tudor, J.; Barlow, S.; Drewitt, M. J.; Heyes, S. J.; O'Hare, D. *Chem. Commun.* **1997**, 641.
(12) Lim, M. H.; Blanford, C. F.; Stein, A. *J. Am. Chem. Soc.* **1997**, *119*, 4090−4091.
(13) Lim, M. H.; Blanford, C. F.; Stein, A. *Chem. Mater.* **1998**, *10*, 467−470.
(14) VanRhijn, W. M.; DeVos, D. E.; Sels, B. F.; Bossaert, W. D.; Jacobs, P. A. *Chem. Commun.* **1998**, 317−318.
(15) Burkett, S. L.; Sims, S. D.; Mann, S. *Chem. Commun.* **1996**, 1367−1368.
(16) Macquarrie, D. J. *Chem. Commun.* **1996**, 1961−1962.
(17) Moller, K.; Bein, T.; Fischer, R. X. *Chem. Mater.* **1999**, *11*, 665−673.
(18) Wen, J.; Wilkes, G. L. *Chem. Mater.* **1996**, *8*, 1667−1681.
(19) Wilkes, G. L.; Orler, B.; Huang, H. *Polym. Prepr.* **1985**, *26*, 300.
(20) Schmidt, H. *J. Non-Cryst. Solids* **1985**, *73*, 681−691.

10.1021/cm9903935 CCC: $18.00
Published on Web 10/09/1999

There are many approaches to the sol−gel synthesis of hybrid materials, most of which involve the combination of two or more precursor species, as has been done for the direct synthesis of hybrid versions of MCM-41. We report an approach based on the use of a single precursor, such as 1,2-bis(triethoxysilyl)ethane (BTSE) or 1,2-bis(triethoxysilyl)ethylene (BTSEY). The advantages of using a double trialkoxylsilyl precursor are that bonding is already established between the organic and inorganic phases and the stoichiometry between silicon and carbon in the framework is assured. The precursor is hydrolyzed and condensed in the presence of cetyltrimethylammonium bromide (CTAB) surfactant micelles as is done in MCM-41 syntheses. Products have been designated UOFMNs (unified organically functionalized mesoporous networks). Unlike surface modified mesoporous materials, the framework of a UOFMN material itself consists of inorganic and organic components which are covalently linked. Organic functionalization of the framework provides an opportunity for further modification.

Experimental Section

Chemicals. BTSE and BTSEY (~80% trans isomer) were obtained from Gelest, Inc., NaOH, HCl (37%), TEOS, methyl alcohol, CH_2Cl_2, and CTAB were obtained from Aldrich, and H_2SO_4 was obtained from Mallinckrodt. All chemicals were used as received without further purification. Water used in all syntheses was distilled and deionized to 17.5 MΩ cm.

Synthesis of UOFMN-1 (Si−CH_2CH_2−Si). UOFMN-1 materials were synthesized from mixtures of typical molar composition 1.00 CTAB:3.38 BTSE:1.32 H_2SO_4:6.42 NaOH:1215−1620 H_2O. CTAB was dissolved in water by stirring and mild heating in a closed polypropylene bottle, and the pH lowered to ca. 2 by addition of H_2SO_4. BTSE was added, and the mixture was stirred for up to 2 h to hydrolyze the precursor. NaOH was then added to raise the pH level to 11 or greater; precipitation occurred instantly at pH 9. The mixture was stirred for 1 day and allowed to settle for 1 day. Reactions were also performed in which BTSE was not hydrolyzed in acidic solution. NaOH was added to raise the pH to ≥11; precipitation occurred in the stirring mixture over 3−4 h. Products were collected by suction filtration, washed with water, and dried in air at room temperature. The template was removed by a modified solvent extraction process. A 2 g sample of product was refluxed in 3 mL of 37 wt % HCl/200 mL of methanol for 1 day, collected by suction filtration, washed with water, and dried in air at room temperature. Removal of surfactant was observed by FTIR spectroscopy. The alkyl C−H stretching vibration bands at 2925 cm^{-1} (asymmetric) and 2850 cm^{-1} (symmetric) decreased in intensity, but did not disappear completely. Alkyl stretching bands for CTAB are indistinguishable from those of the ethane groups in BTSE, though they can be distinguished by NMR. Products from syntheses in which the precursor was hydrolyzed in acid are designated UOFMN-1a. UOFMN-1b resulted from a synthetic mixture which did not contain acid.

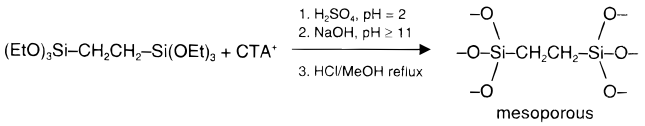

Synthesis of UOFMN-2 (Si−CH=CH−Si). UOFMN-2 materials were synthesized from mixtures of typical molar composition 1.00 CTAB:3.37 BTSEY:0.819 H_2SO_4:1.41 NaOH:1215−1620 H_2O. The synthesis and surfactant removal protocol was analogous to that of UOFMN-1. The extraction time for one sample was extended over 8 days to attempt complete removal of the surfactant. The reaction was also performed without hydrolysis of the precursor in acidic solution prior to addition of the base. Precipitation occurred within 1 h. UOFMN-2a refers to a material from a synthesis mixture which included acid; no acid was included in the synthesis of UOFMN-2b.

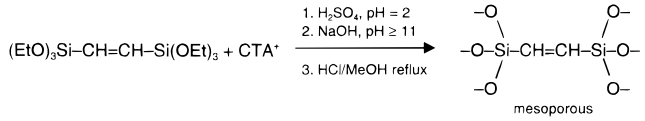

Synthesis of MCM-41-RT. Pure silica analogues of UOFMN-1a (1.00 CTAB:6.75 TEOS:1.57 H_2SO_4:3.83 NaOH:1250−1620 H_2O) and UOFMN-1b (1.00 CTAB:6.75 TEOS:0.248 NaOH:1250−1620 H_2O) with MCM-41 structures were synthesized at room temperature. The synthetic procedure of UOFMN-1 was copied, using TEOS in place of an organosilane precursor. The pH level was raised to 9 with NaOH. The surfactant was removed either by refluxing in HCl/methanol as described for UOFMN-1 or by calcination. For calcination, the temperature was raised at 1.5 °C/min to 550 °C under flowing nitrogen and then held at 550 °C for 7 h under flowing air.

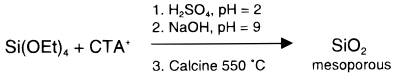

Bromination of Ethylene in UOFMN-2 [Si−CH(Br)−CH(Br)-Si]. A sample of UOFMN-2a (surfactant extracted) was placed on a watch glass set inside a beaker. Several drops of bromine were added to the beaker, avoiding direct contact with the UOFMN-2a sample. The beaker was covered with Parafilm to contain the Br_2 gas. UOFMN-2a was exposed to the gas over 18 h. The product was washed with CH_2Cl_2 to remove adsorbed bromine, followed by a washing with water. Removal of adsorbed bromine could be followed visibly, as the product changed from an orange color to

(21) Prasad, P. N. *Polymer* **1991**, *32*, 1746.
(22) Avnir, D.; Levy, D.; Reisfeld, R. *J. Phys. Chem.* **1984**, *88*, 5956.
(23) Tanaka, H.; Takahashi, H.; Tsuchiya, J. *J. Non-Cryst. Solids* **1989**, *109*, 164.
(24) Pang, Y.; Samoc., M.; Prasad, P. N. *J. Chem. Phys.* **1991**, *94*, 5282.
(25) Wang, B.; Wilkes, G. L. *J. Macromol. Sci., Pure Appl. Chem.* **1994**, *A31*, 249.
(26) Wen, J.; Wilkes, G. L. *J. Sol-Gel Sci. Technol.* **1995**, *5*, 115.
(27) Schmidt, H. *Mater. Res. Soc. Symp. Proc.* **1990**, *171*, 3.
(28) Kasemann, R.; Schmidt, H. *New J. Chem.* **1994**, *18*, 1117.
(29) Tamami, B.; Betrabet, C.; Wilkes, G. L. *Polym. Bull.* **1993**, *30*, 393.
(30) Tamami, B.; Betrabet, C.; Wilkes, G. L. *Polym. Bull.* **1993**, *30*, 39.
(31) Wen, J.; Wilkes, G. L. *J. Inorg. Organomet. Polym.* **1995**, *5*, 343.

its original white color. The brominated product is designated UOFMN-2aBr.

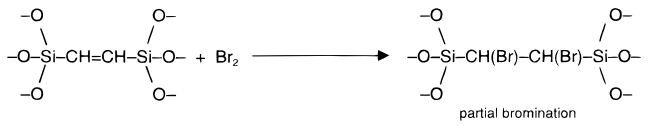

Hydrothermal Treatments of UOFMN-1a and MCM-41-RTa. Samples of UOFMN-1a and MCM-41-RTa were refluxed in water for 17 h to test and compare their hydrothermal stabilities. Powder X-ray diffraction (XRD) experiments were performed, followed by a second and more extensive hydrothermal treatment over 3 days.

Characterization. FTIR spectra were obtained on a Nicolet Magna-IR 760 spectrometer using KBr pellets. XRD experiments were performed on a Siemens D5005 X-ray diffractometer using Cu Kα, $\lambda = 1.540\ 56$ Å. N_2 adsorption−desorption experiments made use of a Micromeritics ASAP 2000 V3.00 sorption analyzer. Samples were dried under vacuum for 2 h at 70 °C and a final pressure of 0.003 mmHg. Solid-state NMR spectra were obtained on a Chemagnetics CMX-400 Infinity spectrometer at room temperature with a 7.5 mm zirconia rotor spinning at 4000 Hz. ^{13}C CP MAS experiments (100.63 MHz, ^1H 90° pulse width 4.5 μs, 5120 acquisitions, pulse delay 2 s) used a hexamethylbenzene standard, and ^{29}Si MAS NMR spectra (single pulse, 79.49 MHz, 90° pulse width 3.00 μs, pulse delay 60 s) used a tetramethylsilane standard. T_1 was determined to be 12 s by an inversion−recovery method using a siliceous MCM-41 sample; 60 s was adequate for obtaining quantitative information. Transmission electron microscopy was carried out on a Philips CM30 transmission electron microscope operating at 300 kV with a LaB_6 filament. Samples were cooled to −150 °C before examination to slow the rate of beam damage. Images were recorded on film. X-ray energy dispersive spectra were recorded in the TEM using an EDAX PV9900 system. Samples for TEM were sonicated for 5 min in ethanol. One drop of the suspended sample was dripped on a holey carbon film supported on a 300 mesh copper grid.

Elemental analysis for Si (wt %) was performed by the Department of Geology, University of Minnesota. Analyses for C, H, N, and Br were performed by Atlantic Microlab, Inc. UOFMN-1a (surfactant present): 19.61% Si, 41.01% C, 7.86% H, 1.79% N, 0.0% Br. UOFMN-1a (most surfactant extracted): 30.37% Si, 20.90% C, 4.03% H, 0.0% N, 0.0% Br. UOFMN-2a (most surfactant extracted): 31.97% Si, 20.10% C, 2.93% H, 0.0% N, 0.0% Br. UOFMN-2aBr: 25.78% Si, 14.01% C, 2.05% H, 0.0% N, 26.64% Br.

Results and Discussion

Structure and Composition. A powder X-ray diffraction pattern for UOFMN-1a typically displayed a low-angle peak at d_{100} spacing = 42 Å (Figure 1a). After extraction of the surfactant template the low-angle peak shifted to $d_{100} = 41$ Å, and the relative peak intensity increased, likely due to a greater density contrast with the surfactant gone (Figure 1b). An XRD pattern for extracted UOFMN-1a also displayed a broad secondary

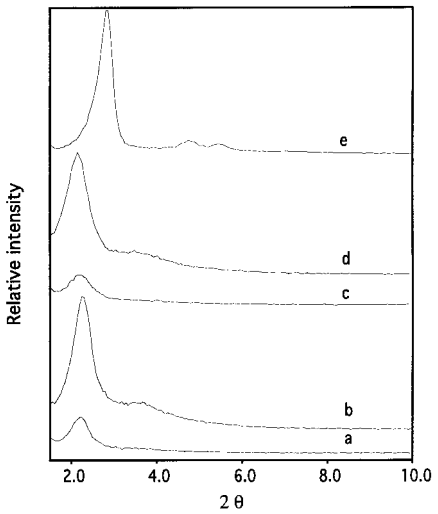

Figure 1. Powder X-ray diffraction patterns of (a) UOFMN-1a as-synthesized, (b) UOFMN-1a surfactant extracted, (c) UOFMN-2a as-synthesized, (d) UOFMN-2a surfactant extracted, and (e) MCM-41-RTa calcined.

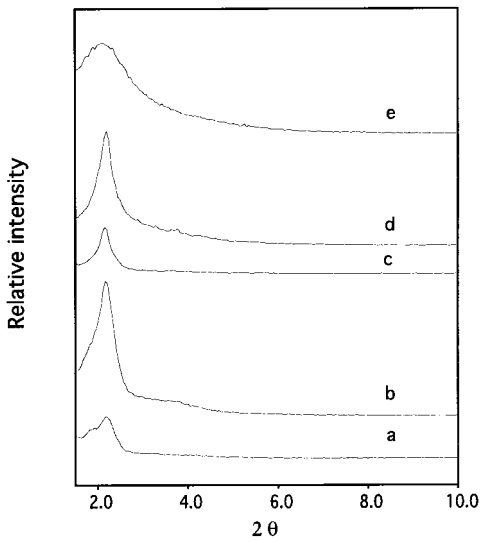

Figure 2. Powder X-ray diffraction patterns of (a) UOFMN-1b as-synthesized, (b) UOFMN-1b surfactant extracted, (c) UOFMN-2b as-synthesized, (d) UOFMN-2b surfactant extracted, and (e) MCM-41-RTb calcined.

feature where (110) and (200) reflections would be expected for a hexagonally ordered material such as MCM-41. However, the absence of resolved peaks indicated that any structural order of the material did not extend over a long range. The XRD pattern for UOFMN-1b (Figure 2a) also had a low-angle reflection at $d_{100} = 42$ Å. Peak intensity increased after template extraction, and a broad feature appeared similar to that displayed in a UOFMN-1a pattern (Figure 2b). This feature, though, was not as pronounced as that of UOFMN-1a.

A powder X-ray diffraction pattern for UOFMN-2a displayed a low-angle peak at d_{100} spacing = 42 Å (Figure 1c). The peak increased in intensity after template extraction, but did not shift (Figure 1d). A broad feature similar to that of UOFMN-1 products also appeared. UOFMN-2b yielded a peak at $d_{100} = 42$ Å, which shifted to $d_{100} = 41$ Å and increased in intensity after template removal (Figure 2c,d). A secondary reflection was not observed.

X-ray diffraction showed that as-synthesized MCM-41-RT products were less stable to solvent extraction than their hybrid framework analogues and also less stable than MCM-41 samples prepared at higher temperature.[32] XRD patterns of MCM-41-RTa (TEOS acid prehydrolyzed) and MCM-41-RTb (base only) after the solvent extraction process displayed very little structural order. Calcination was necessary to obtain a stable product that showed order in an XRD pattern. Calcined MCM-41-RTb (Figure 2e) yielded a poorly resolved low-angle peak located at $d_{100} = 43$ Å. The pattern for calcined MCM-41-RTa (Figure 1e) was typical of a material with hexagonal order, exhibiting (100), (110), and (200) reflections ($d_{100} = 32$ Å). TEOS was prehydrolyzed with acid in the synthesis of MCM-41-RTa; raising the pH with base caused a rapid precipitation which resulted in a more stable and ordered product.

Cryo-TEM at −150 °C was necessary to obtain images of UOFMN materials. The hybrid frameworks did not survive long under the electron beam at room temperature, shrinking in seconds until their structure disappeared. UOFMN-1a had a fine particle morphology with no regular shape (Figure 3a). TEM micrographs suggested the existence of wormlike channels (Figure 3a,b). Such a channel system is reminiscent of MSU-X materials synthesized by Pinnavaia and co-workers.[33,34] MSU-X materials yielded single XRD peaks, which were believed to be reflections of their narrow pore size distributions, or regular channel dimensions. This seemed to be the case with UOFMN materials. XRD patterns of acid-prehydrolyzed UOFMN-1a products had a secondary reflection that was more pronounced than that of UOFMN-1b materials synthesized without acid. This suggested a slightly longer range order, something that was too difficult to verify with wormlike channels. However, long range order may not necessarily be important for diffusion in a high surface area support application.

A ^{29}Si MAS NMR spectrum of UOFMN-1a displayed two peaks, located at −58 and −64 ppm (Figure 4a). These resonances were assigned to T^2 [$RSiO_2(OH)$] and T^3 ($RSiO_3$) Si atoms. The presence of T^2 Si atoms was indicative of incomplete condensation of the organosilane precursor; unreacted silanol groups were still present. A ^{13}C CP MAS NMR spectrum (Figure 5a) displayed a strong resonance at 5 ppm which was attributed to ethane carbon atoms in the framework. Peaks due to surfactant carbon atoms (32, 30, 23, and 13 ppm) were of much smaller relative intensity. A resonance at 49 ppm was assigned to carbon atoms from methanol that was probably trapped during the solvent extraction.

The T^2 and T^3 resonances in the ^{29}Si MAS NMR spectrum of UOFMN-2a were located upfield of those for UOFMN-1a at −75 and −83 ppm, respectively (Figure 4b). The ethylene carbon atoms resonated strongly at 146 ppm on a ^{13}C CP MAS NMR spectrum (Figure 5b). Trapped methanol (49 ppm) and some surfactant (10−32 ppm) were still present.

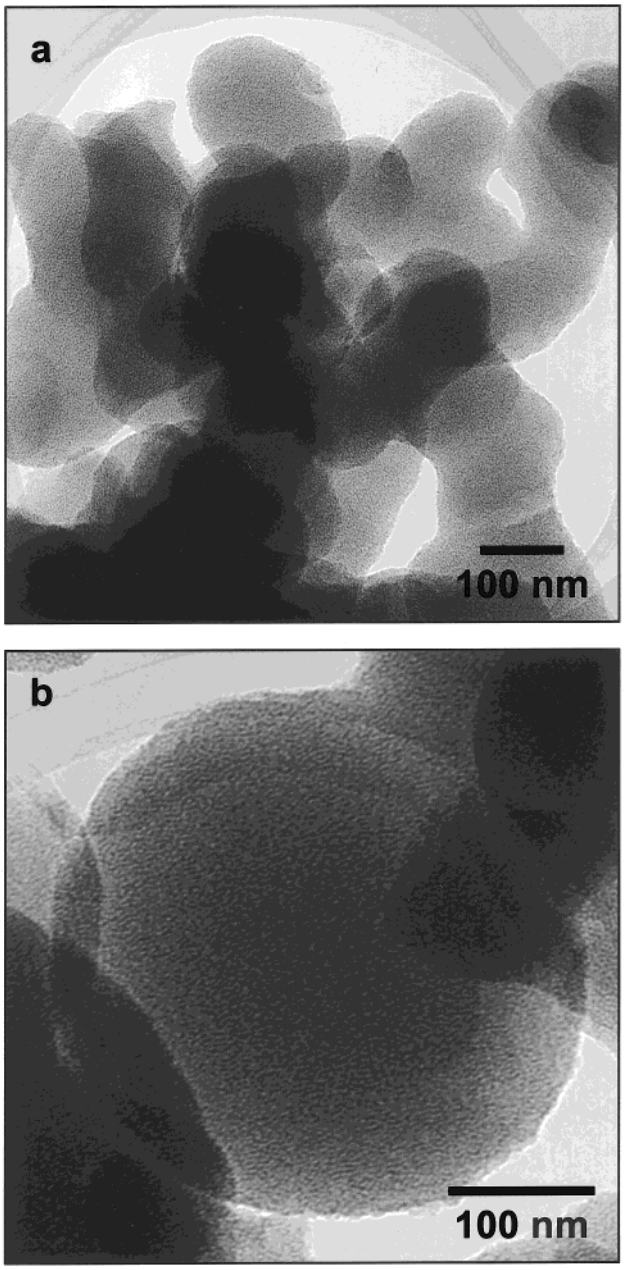

Figure 3. Cryogenic-TEM micrographs of UOFMN-1a (surfactant extracted) taken at −150 °C: (a) view of several particles showing morphology, (b) view of one particle.

Surface Area, Pore Volume, and Pore Wall Thickness. A nitrogen adsorption experiment performed on a surfactant-extracted UOFMN-1a sample yielded a Brunauer−Emmett−Teller (BET) calculated surface area of 1234 m^2/g. The Barrett−Joyner−Halenda (BJH) absorption pore volume was 0.656 cm^3/g. This was comparable to a sample of calcined MCM-41-RTa with its BET surface area of 1225 m^2/g and BJH pore volume of 0.739 cm^3/g. UOFMN-2a had a surface area of 1210 m^2/g and pore volume of 0.934 cm^3/g. Results are summarized in Table 1. The adsorption experiments produced type IV isotherms characteristic of mesoporous materials and narrow pore size distributions (Figure 6). A difference between the hybrid inorganic/organic and pure silica frameworks was indicated by pore size calculations. Solvent-extracted UOFMN-1a, UOFMN-2a, and calcined MCM-41-RTa had respective BJH

(32) Chen, C.-Y.; Li, H.-X.; Davis, M. E. *Microporous Mater.* **1993**, *2*, 17−26.
(33) Bagshaw, S. A.; Prouzet, E.; Pinnavaia, T. J. *Science* **1995**, *269*, 1242−1244.
(34) Bagshaw, S. A.; Pinnavaia, T. J. *Angew. Chem., Int. Ed. Engl.* **1996**, *35*, 1102−1105.

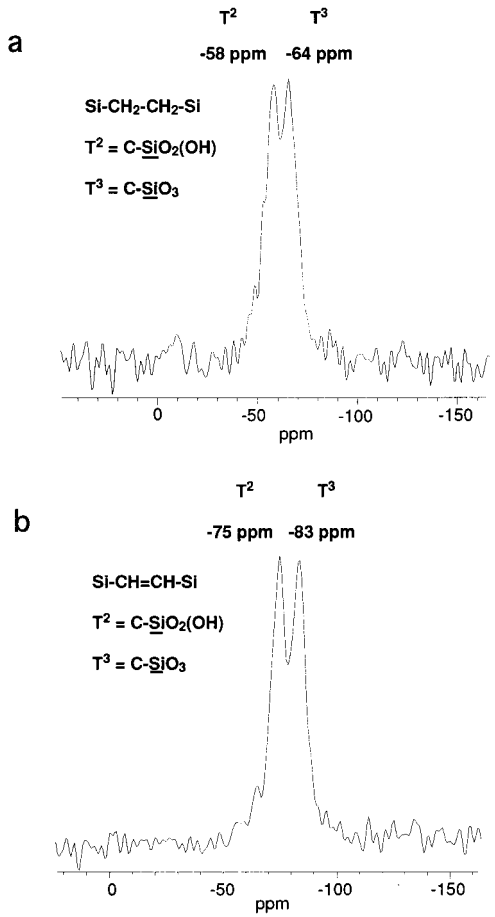

Figure 4. ^{29}Si MAS NMR spectra of (a) UOFMN-1a (surfactant extracted) and (b) UOFMN-2a (surfactant extracted).

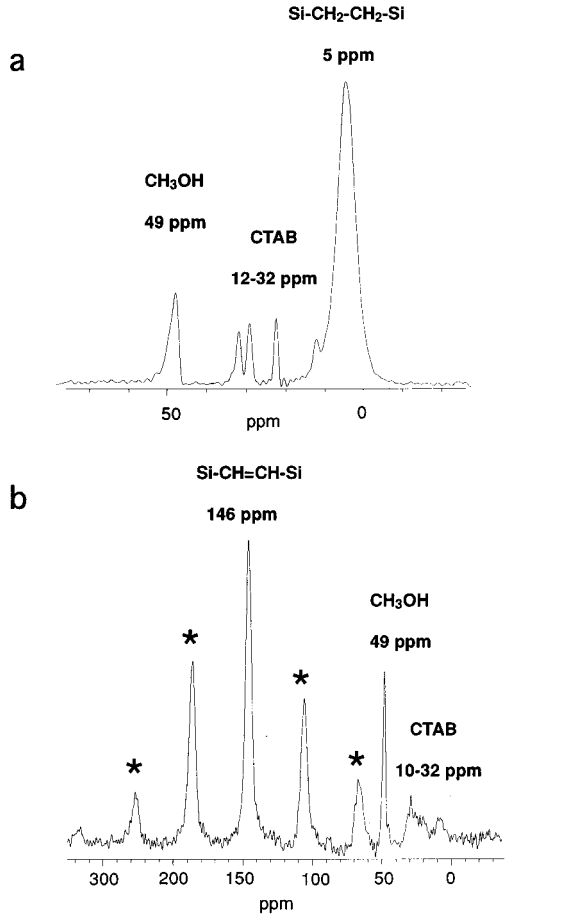

Figure 5. ^{13}C CP MAS NMR spectra of (a) UOFMN-1a (surfactant extracted) and (b) UOFMN-2a (surfactant extracted). The asterisks denote spinning sidebands.

absorption pore sizes of 22, 24, and 21 Å, though the *d* spacings of their (100) XRD peaks differed by as much as 10 Å. Pore wall thicknesses can be estimated by subtracting the pore size from the unit cell value a_0 determined from the d_{100} spacing, where $a_0 = 2d_{100}/\sqrt{3}$. The calculation yielded pore wall thickness values of 16 Å for MCM-41-RTa, 25 Å for UOFMN-1a, and 24 Å for UOFMN-2a. Though the absolute value of the wall thickness depends on the model used for the pore size calculation, the trend in this series indicates that UOFMN materials had thicker pore walls than their pure silica mesoporous analogues templated by the same surfactant.

UOFMN hybrid molecular sieves share the high surface areas and pore volumes of MCM-41, though they do not have the long-range structural order. In contrast to previous organically functionalized MCM-41 materials, the stoichiometry between silicon and carbon in the framework is assured. Another notable difference is the thicker pore wall of a UOFMN material. This may be due to the larger size of a hydrolyzed double trialkoxysilane monomer compared to that of a hydrolyzed tetraalkoxysilane monomer. The formation of MCM-41 in basic solution is governed by electrostatic charge matching between cationic surfactant headgroups and anionic silicate monomers or oligomers. Larger monomeric or oligomeric species would likely condense into thicker walls.

The condensation of silicate species is strongly influenced by pH, a condition which should be considered in understanding the formation of the UOFMN and MCM-41 products reported here. Siloxane precursors were stirred in acidic surfactant solutions prior to precipitation by base addition. The pH of an acidic mixture was at or below a value of 2, the isoelectric point (IEP) of silica where silica species have a surface charge of zero.[35] The IEP may be higher for alkyl substituted precursors (BTSE and BTSEY), as electron providing groups are expected to reduce the acidity of the corresponding silanols.[36,37] The hydrolyzed TEOS species are neutral or cationic. Condensation, or siloxane polymerization, under this condition is believed to occur by protonation of silanols followed by electrophilic attacks on the Si atoms by neutral silicate species (≡Si−OH or ≡Si−OR).[36,37] Less highly condensed sites, those that are relatively electron rich, are favored by this process. This leads to more extended, branched structures than those obtained under basic conditions. Charge matching between cationic silicate species (monomers or oligomers) and cationic surfactant headgroups is mediated by anions, a weaker interaction that is not as likely to terminate wall structure growth and allow silicate species to further polymerize. Adding NaOH rapidly

(35) Brinker, C. J.; Scherer, G. W. *Sol−Gel Science*; Academic Press: Boston, 1990.
(36) Brinker, C. J. *J. Non-Cryst. Solids* **1988**, *100*, 31−50.
(37) Coltrain, B. K.; Kelts, L. W. In *The Chemistry of Hydrolysis and Condensation of Silica Sol−Gel Precursors*; Bergna, H. E., Ed.; American Chemical Society: Washington, DC, 1994; Vol. 234, pp 403−418.

Table 1. Unit Cell and N_2 Adsorption Data

sample	d_{100} (Å)	BET surface area (m^2/g)	BJH ads pore vol (cm^3/g)	BJH ads pore size (Å)	wall thickness[a] (Å)
UOFMN-1a (solvent extracted)	41	1234	0.656	22	25
UOFMN-2a (solvent extracted)	42	1210	0.934	24	24
UOFMN-2aBr	42	897	0.673	24	24
MCM-41-RTa (calcined)	32	1225	0.739	21	16

[a] Calculation: a_0 − pore size, where $a_o = 2d_{100}/\sqrt{3}$.

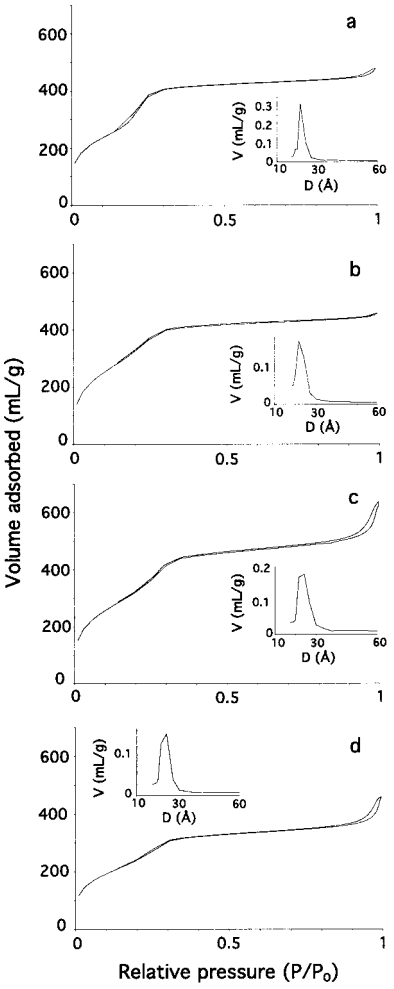

Figure 6. N_2 adsorption−desorption isotherms of (a) MCM-41-RTa, (b) UOFMN-1a, (c) UOFMN-2a, and (d) UOFMN-2aBr (brominated UOFMN-2a). The insets show BJH adsorption pore size distributions of the corresponding samples. v = pore volume, and D = pore diameter.

should cause the oligomers to become anionic, resulting in more direct positive−negative charge matching between silicate and surfactant species and terminating wall growth.

Hydrothermal Stability. The structure of UOFMN-1a could survive boiling water for 17 h with only little damage, as its XRD peak decreased slightly in intensity (Figure 7c). The structural order of MCM-41-RTa suffered more damage, though its (100) reflection was still prominent (Figure 7a). Structural damage was much more severe after 3 more days of reflux in water. The pore structure of MCM-41-RTa collapsed (Figure 7b), but UOFMN-1a still produced a distinct low-angle XRD peak (Figure 7d). Hydrothermal instability of porous silica is believed to result from a low degree of silicate condensation or cross-linking, providing silanol groups which are weak points for attack by water. The hybrid UOFMN material exhibited a better hydrothermal

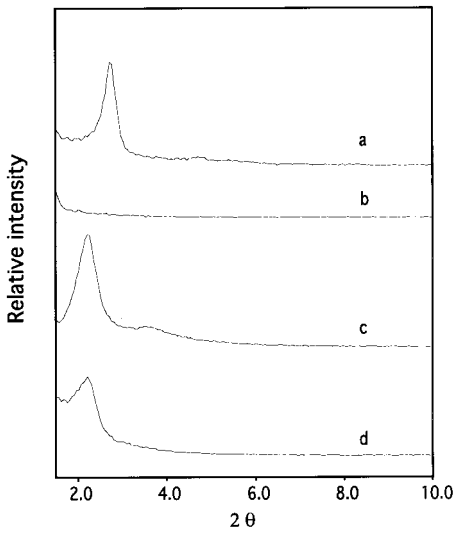

Figure 7. Powder X-ray diffraction patterns of (a) MCM-41-RTa hydrothermally treated for 17 h, (b) MCM-41-RTa hydrothermally treated for another 3 days, (c) UOFMN-1a hydrothermally treated for 17 h, and (d) UOFMN-1a hydrothermally treated for another 3 days.

stability than the pure silica MCM-41, though ^{29}Si MAS NMR spectra implied that there should have been a significant amount of silanol groups present. The greater hydrothermal stability of UOFMN-1a is believed to result from its thicker pore walls and hydrophobicity imparted by the organic components in the framework.

Hydrophobicity and Organic Absorption. Adding UOFMN-1a to an immiscible mixture of water and chloroform gave a visible demonstration of this property. The sample floated on top of the aqueous phase until the mixture was shaken, after which it was seen with the organic phase. UOFMN-1a, mixed with the chloroform, formed a phase with the appearance of a gel. Further shaking could break off pieces of this agglomerate. This behavior differed from that of pure silica (Silica gel, Merck, grade 60) which, though hydrophobic, merely coated the chloroform phase with little mixing. ^{13}C NMR spectra also showed that UOFMN materials have an affinity for alcohol from the solvent extraction process and still contained a small amount of CTAB surfactant. An acidic reflux for 8 days failed to remove all surfactant from a sample of UOFMN-2a.

Bromination of the Ethylene Linkages in UOFMN-2a. A potential advantage of having a hybrid framework is that it can be modified further, provided the organic groups are functionalizable and accessible. The accessibility of the ethylene bridges in UOFMN-2a was tested by a gas-phase bromination reaction. Bromination of alkenyl groups within the framework of UOFMN-2a did not have much of an effect on its XRD pattern. The low-angle peak (d_{100} = 42 Å) and a broad secondary feature were still present, though with a small decrease in peak intensity. Bromination of the

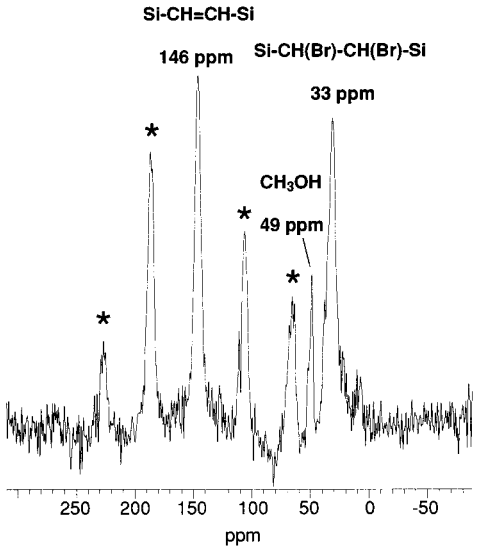

Figure 8. ^{13}C CP MAS NMR spectrum of UOFMN-2aBr (brominated UOFMN-2aBr). The asterisks denote spinning sidebands.

UOFMN-2a framework was observed by ^{13}C CP MAS NMR (Figure 8). After exposure to the halogen, a spectrum showed a peak at 33 ppm which was attributed to brominated carbon; the existence of a peak at 146 ppm indicated that bromination was not complete within 18 h or that not all the ethylene groups in the framework were accessible for bromination. In contrast, MCM-41 containing vinyl groups at the surface could be completely brominated in a gas-phase reaction within 40 min.[38]

Cryo-TEM images were obtained for brominated UOFMN-2aBr. Bromination was apparently not detrimental to porosity, as the wormlike channels were still present (Figure 9). An X-ray energy dispersive spectrum verified that a relatively large amount of bromine was present. N_2 adsorption showed a decrease in pore volume (from 0.934 to 0.673 cm^3/g) and surface area (from 1210 to 897 m^2/g) after bromination with no decrease in pore size. A type IV isotherm and narrow pore size distribution were obtained (Figure 6d).

^{13}C CP MAS NMR proved that many of the ethylene components could be brominated with little damage to the structure of the material as seen by XRD and TEM. UOFMN-2aBr was reactive itself as a source of bromide. Stirring a sample of UOFMN-2aBr in aqueous $AgNO_3$ produced AgBr which gave a crystalline XRD pattern with narrow peaks. XRD also showed that a low-angle structural peak for UOFMN-2a remained. A ^{13}C CP MAS NMR spectrum of the brominated product after the $AgNO_3$ treatment was largely unchanged compared to its earlier spectrum. The only noteworthy difference was a new resonance at 128 ppm, a region where alkenyl carbons resonate. The possibility of Si−C bond breakage cannot be ruled out at this stage. Bromination of UOFMN-2a and the resulting product's reactivity and structural changes will be investigated further in the future. The opportunity to tune the frameworks makes UOFMN-type materials attractive as potential high surface area supports for catalysis or other chemical processes.

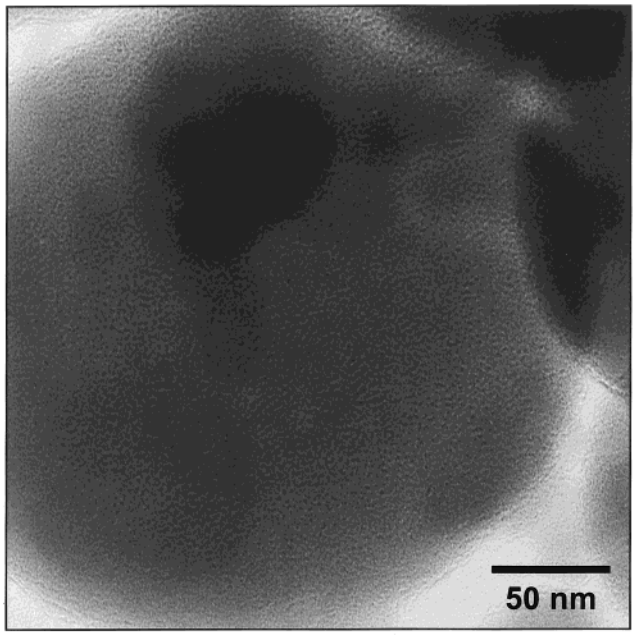

Figure 9. Cryogenic-TEM (−150 °C) micrograph of UOFMN-2aBr.

Conclusion

Mesoporous materials designated UOFMN have been synthesized with frameworks composed of inorganic and organic components that are covalently linked to each other. The synthesis uses a single precursor that consists of two trialkoxysilyl groups connected by an organic bridge and ionic surfactant as a space filler. UOFMN products are comparable to MCM-41 in that they have high surface areas (ca. 1200 m^2/g) and narrow pore size distributions, though their pore walls are considerably thicker. Their pore structures consist of wormlike channels templated by the CTAB surfactant. A hybrid UOFMN mesostructure is more hydrothermally stable than a pure silica MCM-41 analogue prepared at room temperature, possibly due to a greater hydrophobicity. UOFMN materials are also able to absorb organic compounds, a property which will be studied and quantified in the future. A UOFMN material with alkenyl bridges between silicon atoms was brominated with little or no damage to the pore structure. The brominated UOFMN product was itself reactive as a bromide source.

Acknowledgment is made to 3M, Dupont, the David and Lucille Packard Foundation, the McKnight Foundation, the National Science Foundation (NSF) (Grant DMR-9701507), the MRSEC Program of the NSF under Award Number DMR-9809364, and the Office of the Vice President for Research and Dean of the Graduate School of the University of Minnesota for support of this research. C.F.B. thanks the Center for Interfacial Engineering at the University of Minnesota for a CIE-NSF graduate fellowship. We thank P. K. Isbester for assistance with obtaining NMR spectra.

CM9903935

(38) Lim, M.; Stein, A. *Mater. Res. Soc. Symp. Proc.* **1998**, *519*, 89−94.